Investigations into the impact of the lower boundary condition on the reflected solar radiance field

Katja Hungershöfer and Thomas Trautmann

Summary

It is presented how the original isotropic boundary condition in a Gauss-Seidel radiative transfer model is generalized to describe an angular dependent surface reflection. A symmetry about the plane of incidence is assumed since the general case of an arbitrary non-symmetric reflection is to costly. As a result using Hapke's BRDF the upward radiance at the surface and the top of the atmosphere are discussed and compared to the results with the original isotropic boundary condition. In addition we discuss the impact of Rayleigh scattering and aerosol extinction on the reflected solar radiance field.

Zusammenfassung

Es wird dargestellt wie die untere Randbedingung in unserem Gauss-Seidel Strahlungstransportmodell erweitert wird, um eine richtungsabhängige Reflexion beschreiben zu können. Da die Beschreibung einer asymmetrischen Bodenreflexion zu aufwendig wäre, beschränken wir uns dabei auf den Fall, bei dem die Reflexion symmetrisch bezüglich der Einfallsebene ist. Als Ergebnisse werden die aufwärtsgerichtete Strahldichte unmittelbar am Erdboden und am Atmosphärenoberrand diskutiert und mit den Ergebnissen für die ursprünglich isotrope Reflexion verglichen. Außerdem wird auf den Einfluß der Rayleigh Streuung und der Extinktion durch die Aerosolpartikel auf das reflektierte solare Strahldichtefeld eingegangen.

1. Introduction

All natural surfaces like bare soils, vegetation canopy or oceans reflect the light anisotropically. Perhaps the best known examples are the sun glint on water surfaces or the hot spot effect, which results in a high reflectance, if the viewing direction and the direction of the light source are identical.

The reflection of the solar light at the earth's surface plays an important role in the remote sensing of the atmosphere, because the measured radiance at the top of the atmosphere may contain a signal from the surface. In order to use satellite measurements, a radiative transport model which describes the different interactions between the solar radiation and the atmosphere is needed. With the help of suitable methods, such models can be inverted against the satellite measurements to determine selected properties of the atmosphere. Because of the multiple scattering of radiation between the atmosphere and the surface, a reliable surface reflexion described by the lower boundary condition in these models plays an essential role in the retrieval. On one hand, an accurate description of the surface reflection leads to a better interpretation of the satellite measurements in terms of the atmospheric properties and on the other hand the models with a realistic lower boundary can be inverted to retrieve key parameters of the surface such as the leaf area index or the soil roughness (Bréon et al., 1997) which may be useful for land cover classifications.

Of special interest are radiative transfer models with a realistic surface reflection for mod-

ern instruments like the ATSR-2 (Along-Track Scanning Radiometer), POLDER (Polarization and Directionality of earth Reflectances) or MISR (Multiangle Imaging SpectroRadiometer), which measure the radiance of a surface pixel under different viewing directions simultaneously. With the MISR instrument for example one is able to separate the aerosol signal from that of the surface reflectance and determine the aerosol properties (Kaufman et al., 2002). More details about the advantages of multi-angle remote sensing can be found in Diner et al. (1999).
Our own radiative transfer model named Gauss-Seidel after the technique used to solve the radiative transfer equation, is very versatile. It has been used together with the forward-adjoint perturbation theory (Trautmann et al., 1992; Trautmann and Box, 1995) and for the ozone retrieval from satellite measurements (Landgraf et al., 2001; Landgraf and Hasekamp, 2002). For the ozone retrieval, a vector radiative transfer model is also available (Hasekamp and Landgraf, 2002) and a pseudo-spherical approximation can be used instead of the plane-parallel assumption (Walter et al., 2002). Since the earth's surface has simply been treated as Lambertian surface, where the reflection does not vary with viewing or illuminating directions in all the applications given above, we have extended the lower boundary condition in the Gauss-Seidel code to make this model a more realistic, angular dependent surface reflection. This is described and verified with results in the following sections.

2. Theory

The basic equation governing the radiative transfer of the solar spectral diffuse radiance L in a plane-parallel and horizontally homogeneous atmosphere is generally written in the form

$$\begin{aligned} \mu \, \frac{\mathrm{d}L(\tau,\mu,\phi)}{\mathrm{d}\tau} = \; & - \; L(\tau,\mu,\phi) + \frac{\widetilde{\omega}}{4\pi} \int_{-1}^{1} \int_{0}^{2\pi} p(\tau,\cos\Theta) \; L(\tau,\mu',\phi') \; \mathrm{d}\phi' \; \mathrm{d}\mu' \\ & + \; \frac{\widetilde{\omega}}{4\pi} \; \pi F_0 \; p(\tau,\mu_0,\phi_0;\mu,\phi) \; \exp(-\tau/\mu_0) \end{aligned} \tag{1}$$

where μ is the cosine of the zenith angle θ and ϕ is the azimuth angle with respect to the solar beam positioned at ϕ_0. The prime is used to separate the incident directions from the scattered ones. τ is the optical depth measured from the top of the atmosphere to a given layer and $\widetilde{\omega}$ is the single scattering albedo describing the relative importance of the absorption to the total extinction. πF_0 is the solar spectral irradiance at the top of the atmosphere and the phase function p describes the angular dependence of the scattering. Here, as usual, we assume that p depends only on the scattering angle Θ between the incident and emergent direction. In this case the phase function can be expanded in Legendre polynomials P_l

$$p(\tau, cos\Theta) = \sum_{l=0}^{\Lambda} \; \beta_l(\tau) \; P_l(cos\Theta) \tag{2}$$

with the expansion coefficients β_l

$$\beta_l = \frac{2l+1}{2} \int_{-1}^{1} \; p(cos\Theta) \; P_l(cos\Theta) \; \mathrm{d}cos\Theta \; . \tag{3}$$

Together with an expansion of the radiance in a Fourier series in azimuth

$$L(\tau,\mu,\phi) = \sum_{m=0}^{\Lambda} (2-\delta_{0,m})\ L^m(\tau,\mu)\ \cos(m\phi) \tag{4}$$

this finally leads to a splitting of equation (1) into $\Lambda+1$ independent equations for the single Fourier modes (e.g. Liou, 1992)

$$\mu\ \frac{\mathrm{d}L^m(\tau,\mu)}{\mathrm{d}\tau} = -L^m(\tau,\mu) + J^m(\tau,\mu)\ , \quad m = 0,1,\ldots\Lambda \tag{5}$$

with the source function given by

$$\begin{aligned} J^m(\tau,\mu) \;=\; & \frac{\omega_0}{4\pi}\ \pi F_0\ \sum_{l=m}^{\Lambda}\ \beta_l^m\ P_l^m(\mu)\ P_l^m(\mu_0) e^{-\tau/\mu_0} \\ & + (1+\delta_{0,m})\ \frac{\omega_0}{4}\ \sum_{l=m}^{\Lambda}\ \beta_l^m\ P_l^m(\mu)\ \int_{-1}^{1}\ P_l^m(\mu')\ L^m(\tau,\mu')\ \mathrm{d}\mu'\ . \end{aligned} \tag{6}$$

For this kind of differential equations, a formal solution can be calculated. After separating the upward ($L_\uparrow^m(\tau,\mu) := L^m(\tau,\mu<0)$) and downward ($L_\downarrow^m(\tau,\mu) := L^m(\tau,\mu>0)$) radiance we have

$$L_\downarrow^m(\tau,\mu) = L_\downarrow^m(\tau=0,\mu)\ e^{-\tau/\mu} + \frac{1}{\mu}\ \int_0^\tau J_\downarrow^m(\tau',\mu)\ e^{-(\tau-\tau')/\mu}\ \mathrm{d}\tau'\ , \tag{7}$$

$$L_\uparrow^m(\tau,\mu) = L_\uparrow^m(\tau_N,\mu)\ e^{-(\tau_N-\tau)/\mu} + \frac{1}{\mu}\ \int_\tau^{\tau_N} J_\uparrow^m(\tau',\mu)\ e^{-(\tau'-\tau)/\mu}\ \mathrm{d}\tau'\ . \tag{8}$$

Note that $\mu<0$ and $\mu>0$ describe the radiation in the upward and downward directions, respectively, since θ is measured from the positive τ-axis.
In order to solve these equations for a vertically inhomogeneous atmosphere the atmosphere is divided into several homogeneous layers following Herman and Browning (1965), in which the source functions $J_\downarrow^m(\tau',\mu)$ and $J_\uparrow^m(\tau',\mu)$ are assumed to be independent of the optical depth. The μ-integration in the source term is solved with the Gauss-Lobatto quadrature with 32 discrete streams μ_i and the discretization of μ leads to a system of linear equations which are then solved with the iteration procedure of Gauss-Seidel as described in Landgraf et al. (2001) and Hungershöfer (2001). Beside this, two boundary conditions are needed. At the top of the atmosphere we assume that no downward diffuse radiation exists

$$L_\downarrow^m(\tau=0,\mu) = 0\ . \tag{9}$$

In order to describe the reflection of radiation by an opaque surface, we use the spectral bidirectional reflectance distribution function (BRDF) $\rho(\theta',\phi';\theta,\phi)$ (Nicodemus, 1970), which is defined as

$$\rho(\theta',\phi';\theta,\phi) = \frac{\pi\ \mathrm{d}L(\theta',\phi';\theta,\phi)}{L(\theta',\phi')\ \cos\theta'\ \mathrm{d}\Omega'} \tag{10}$$

where (θ',ϕ') and (θ,ϕ) are the zenith and azimuth angles of the incident and reflected direction. Here, in contrast to the definition of the BRDF by Siegel and Howell (1981) a

factor π is considered. The unit of the BRDF is $(sr)^{-1}$. The denominator in equation (10) describes the energy incident on a surface element $\mathrm{d}A$ from the direction (θ', ϕ') within the solid angle $\mathrm{d}\Omega'$ and $\mathrm{d}L(\theta', \phi'; \theta, \phi)$ denotes that part of this light, which is reflected into the direction (θ, ϕ), i.e. the BRDF gives that fraction of $L(\theta', \phi') \ \cos\theta' \ \mathrm{d}\Omega'$ which contributes to the reflected spectral intensity in the (θ, ϕ) direction. The entire radiation reflected into the direction (θ, ϕ) can then be found by summing the contribution of $L(\theta', \phi') \ \cos\theta' \ \mathrm{d}\Omega'$ from all incident directions

$$\begin{aligned} L(\theta, \phi) &= \int_{2\pi} \mathrm{d}L(\theta', \phi'; \theta, \phi) \\ &= \frac{1}{\pi} \int_{2\pi} \rho(\theta', \phi'; \theta, \phi) \ L(\theta', \phi') \ \cos\theta' \ \mathrm{d}\Omega' \ . \end{aligned} \tag{11}$$

This directly leads to a lower boundary condition describing an angular dependent surface reflection

$$\begin{aligned} L_{\uparrow}(\tau_N, \mu, \phi) &= \frac{\mu_0}{\pi} \ \pi F_0 \ \rho(\mu_0, \phi_0; \mu, \phi) \ e^{-\tau_N/\mu_0} \\ &\quad + \frac{1}{\pi} \int_0^{2\pi} \int_0^1 \rho(\mu', \phi'; \mu, \phi) \ L_{\downarrow}(\tau_N, \mu', \phi') \ \mu' \ \mathrm{d}\mu' \ \mathrm{d}\phi' \end{aligned} \tag{12}$$

where the reflection of the direct light is described by the first term and the reflection of the diffuse radiation has already been given by equation (11). The quantity τ_N is the optical depth at the surface. Note that the direct solar beam, which reaches the lower boundary and is scattered by the BRDF back into the medium is treated as diffuse radiation thereafter.

The simplest case of a reflection function is a Lambertian reflection where the BRDF is constant, i.e. the amount of reflected light is equal for all directions. In the most general case, e.g. a corn field, the reflection is asymmetric with respect to the plane of incidence. Beside this an additional azimuth angle is needed to describe the alignment of the surface relative to the position of the sun. In case of the corn field, one can choose the direction of the corn rows as reference direction of the surface, for example. Also in the general case, not only the cosine components as in equation (4) but also the sine components have to be considered in the Fourier decomposition of the radiance leading to a second equation system for the sine components analogously to equation (5). What makes this even more complicated is the fact that the first Λ sine and the first $\Lambda + 1$ cosine components are coupled by the lower boundary condition. More details about this can be found in Barichello et al. (1996) and Hungershöfer (2001).

We did not apply the general theory from Barichello et al. (1996), but extended the former isotropic reflection to an angular dependent reflection, which is symmetric about the plane of incidence, i.e. the BRDF depends only on the difference between the azimuth angles of the incident and reflected direction. This enables us to expand the BRDF in a Fourier cosine series just like the radiance in equation (4)

$$\rho(\mu', \mu, \phi - \phi') = \sum_{m=0}^{\Lambda} \rho^m(\mu', \mu) \ \cos[m(\phi - \phi')] \tag{13}$$

where the expansion coefficients ρ^m can be calculated from

$$\rho^m(\mu',\mu) = \frac{1}{\pi}\ \frac{2-\delta_{0,m}}{2}\ \int_{-\pi}^{\pi} \rho(\mu',\mu,\phi-\phi')\ \cos[m(\phi-\phi')]\ \mathrm{d}(\phi-\phi')\ . \tag{14}$$

By inserting equation (13) into equation (12) one finds the lower boundary condition for the individual Fourier components of the radiance that is used in the Gauss-Seidel model

$$\begin{aligned} L^m_{\uparrow}(\tau_N,\mu) &= \frac{\mu_0}{\pi}\ \pi F_0\ \rho^m(\mu_0,\mu)\ e^{-\tau_N/\mu_0} \\ &\quad + (1+\delta_{0,m})\ \int_0^1 \rho^m(\mu',\mu)\ L^m_{\downarrow}(\tau_N,\mu')\ \mu'\ \mathrm{d}\mu'\ . \end{aligned} \tag{15}$$

The needed coefficients $\rho^m(\mu_0,\mu)$ and $\rho^m(\mu',\mu)$ in equation (15) can be calculated from equation (14) if an analytical form of the BRDF is given.
In the literature, various approaches can be found to describe the anisotropy of a surface, including empirical functions (Minnaert, 1941; Cox and Munk, 1954; Walthall et al., 1985; Meister et al., 1996), semi-empirical functions (Pinty and Ramond, 1986; Rahman et al., 1993) and physical models (Hapke, 1981; Verstraete et al., 1990). We have incorporated the BRDF models from Minnaert (1941), Hapke (1981), Verstraete et al. (1990) and Rahman et al. (1993) into our Gauss-Seidel model. All of them obey the important principle of reciprocity (Minnaert, 1941), i.e. the reflectance is unaffected if the direction of incidence and observation is reversed. Here only the results for Hapke's BRDF are shown, which is defined as (Hapke, 1981)

$$\rho(\mu_1,\mu_2,g) = \frac{w}{4}\ \frac{1}{\mu_1+\mu_2}\ [\ (1+B(g))\ p(g) + H(\mu_1)H(\mu_2) - 1\ ] \tag{16}$$

where

$$\begin{gathered} \mu_1 = \cos\theta_1 \quad ; \quad \mu_2 = \cos\theta_2 \\ \cos g = \mu_0\ \mu + \sqrt{(1-\mu_0^2)\ (1-\mu^2)}\ \cos(\phi-\phi_0) \\ p(g) = \frac{1-\Theta_H^2}{(1+\Theta_H^2-2\cdot\Theta_H\cdot\cos(\pi-g))^{3/2}} \\ B(g) = \frac{S(g=0)}{w\cdot p(g=0)}\cdot\frac{1}{1+\frac{1}{h}\ \tan(g/2)} \\ H(x) = \frac{1+2x}{1+2x\ \sqrt{1-w}}\ . \end{gathered}$$

(θ_1,ϕ_1) and (θ_2,ϕ_2) describe the incoming and outgoing directions, respectively and g, the phase angle, is the angle between these two directions. ω is the averaged single scattering albedo of the surface particles. The average phase function of the surface particles, $p(g)$, is computed by a Henyey-Greenstein function (Henyey and Greenstein, 1941), where the asymmetry parameter Θ_H is ranging from -1 (backward scattering) to +1 (forward scattering). The expression of $B(g)$ accounts for the hot spot effect. The amplitude of the hot spot given by the first factor of $B(g)$ is the ratio of the near-surface contribution ($S(g=0)$) to the total particle scattering of the surface at zero phase angle and h characterizes the width of the opposition effect and may be related to the grain size distribution, the porosity and the gradient of compaction with depth (Pinty et al., 1989). In order to use Hapke's model, the four parameters ω, Θ_H, $S(g=0)$ and h have to be known.

3. Model description

We employ an one-dimensional plane-parallel radiative transfer model for a cloudless vertically inhomogeneous atmosphere. Vertical profiles of the air molecules and the absorbing trace gases ozone, nitrogen dioxide and water vapor are taken from the US-standard atmosphere (Anderson et al., 1986). The absorption cross sections of ozone are taken from WMO (1985) and Molina and Molina (1986). For water vapor and nitrogen dioxide data from Rothman (1992) and Mérienne et al. (1995) have been employed.
In the easiest case, only Rayleigh scattering with cross sections from Nicolet (1984) is considered. Additionally the extinction of aerosol particles can be taken into account. Therefore the aerosol extinction coefficient, the single scattering albedo and the phase function for rural aerosol at 0% relative humidity (Shettle and Fenn, 1979) are calculated off-line with a Mie code and are assumed to be constant at all model layers up to a height of two kilometers. To determine the effect of the aerosol loading, the extinction coefficient is scaled with a factor 0.2 or 5 additionally. The extraterrestrial solar flux is taken from WMO (1985) and Woods et al. (1996). For the parameter in Hapke's BRDF, we use the values from Verstraete et al. (1990)

$$\begin{aligned} \omega &= 0.101 \\ \Theta_H &= 0.06 \\ S(g=0) &= 0.589 \\ h &= 0.046 \end{aligned}$$

which have been retrieved from measurements over a clover patch at a wavelength of 448 nm by Woessner and Hapke (1987).

4. Results

In order to examine the influence of the surface reflection, we first look at the spectral upward radiance directly at the earth's surface. Figure 1 shows the results for two different wavelengths and two solar zenith angles (SZA) as a function of the viewing zenith angle in the plane of incidence for a Rayleigh atmosphere. Here as well as in the following figures, positive zenith angles are used for the backscattering direction, where the difference of the azimuth angle between the incident and the outgoing direction is 0°. Negative viewing angles are used when the difference of these azimuth angles is equal to 180°. Since the assumption of a plane-parallel model atmosphere breaks down as the viewing zenith angle approaches 90°, we have only considered viewing angles less than 80°. The plus symbols in Figure 1 indicate the results at the discrete streams μ_i for Hapke's BRDF. Additionally the results for a Lambertian surface with the same albedo as in the Hapke case is given for comparison.
For all four cases in Fig.1, a clear difference between the two reflection types is visible. Whereas the amount of the reflected light is equal for all direction in case of the Lambertian surface, Hapke's function produces a pronounced maximum in the backward direction in the vicinity of the solar zenith angle called backscattering peak. We do not use the term 'hot spot' since this expression should be reserved for the reflectance peak observed within a few degrees of the backscattering direction (Bréon et al., 2001). Altogether more radiation is reflected in the backward direction with Hapke's function and less radiation in the forward direction in comparison to the Lambertian case. It also clears from Fig.1

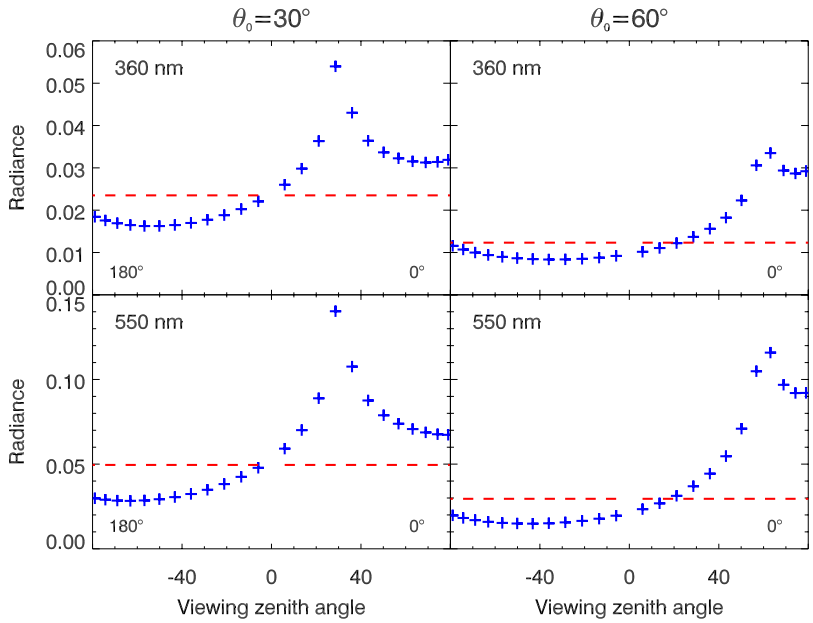

Figure 1: Upward spectral radiance at the surface in $Wm^{-2}sr^{-1}\Delta\nu^{-1}$ as a function of the viewing zenith angle in the plane of incidence for two wavelengths and two SZAs in case of a Rayleigh atmosphere. Positive zenith angles are used for the backward direction. Negative angles indicate the forward direction. As BRDFs Hapke's function (+) and a Lambertian surface with the same albedo (dashed line) are used.

that less light is reflected at 360 nm than at the corresponding SZAs at 550 nm wavelength. Reason for this is the strong wavelength dependence of the Rayleigh scattering (λ^{-4}). At 360 nm, less radiation is able to reach the ground because of the considerably stronger Rayleigh scattering and therefore less radiation can be reflected since the albedo is unchanged. Analogously the decrease of the radiance with increasing SZA in Fig. 1 can be explained.

If aerosol is additionally taken into account, the direct light is more weakend on its way down through the atmosphere. In Figure 2, which shows the upward radiance at the lower boundary at a SZA of 30° for three aerosol optical depths analogously to Fig.1, this can be seen from the decrease of the radiance with increasing optical depth for both reflection types. At low aerosol optical thicknesses, the distinct forward scattering of the aerosol particles also results in a large amount of diffuse radiation reaching the surface from zenith angles around the solar zenith angle. This intensifies the backscattering peak and lowers the light reflected into the other zenith directions in comparison to a Rayleigh atmosphere. This effect is shown in Figure 3, where the normalized results for a Rayleigh atmosphere (Fig.1) and the different aerosol atmospheres (Fig.2) in Hapke's case for a SZA of 30° are given. With increasing aerosol optical depth, the contribution of the diffuse light from directions near the solar zenith angle decreases, because of the multiple scattering, leading to a lower anisotropy in comparison to the Rayleigh atmosphere. Beside this, Fig.3 reveals that the influence of the aerosol on the diffuse radiation is stronger at 360 nm caused by the stronger Rayleigh scattering. If one looks at the contribution of the direct light on the total reflected radiation, which is also shown in Fig.2, one recognizes that at 360 nm, the direct light is more weakend because of the Rayleigh scattering leading to a

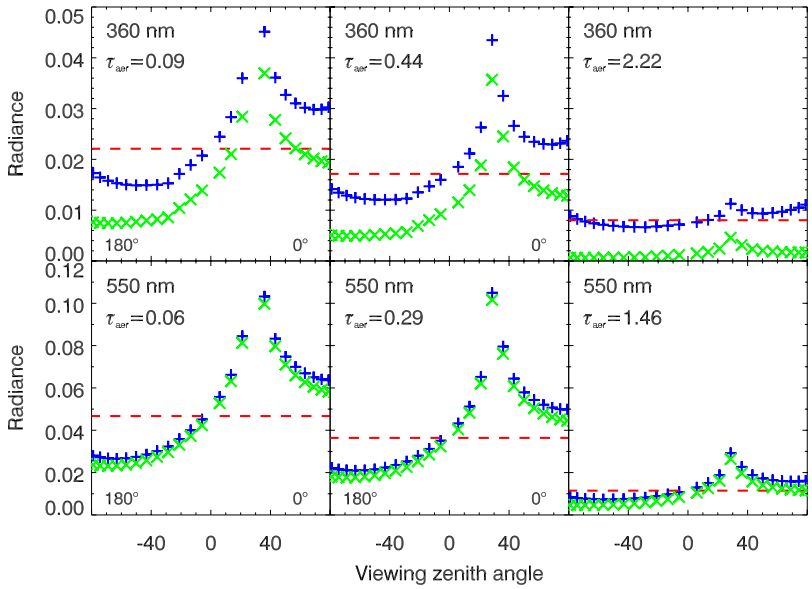

Figure 2: Upward spectral radiance at the surface ($Wm^{-2}sr^{-1}\Delta\nu^{-1}$) as a function of the viewing zenith angle in the principal plane at 30° SZA and three different aerosol optical depths for a Lambertian surface (dashed line) and Hapke's BRDF (+). The crosses show the contribution of the direct light on the total reflected radiation in Hapke's case.

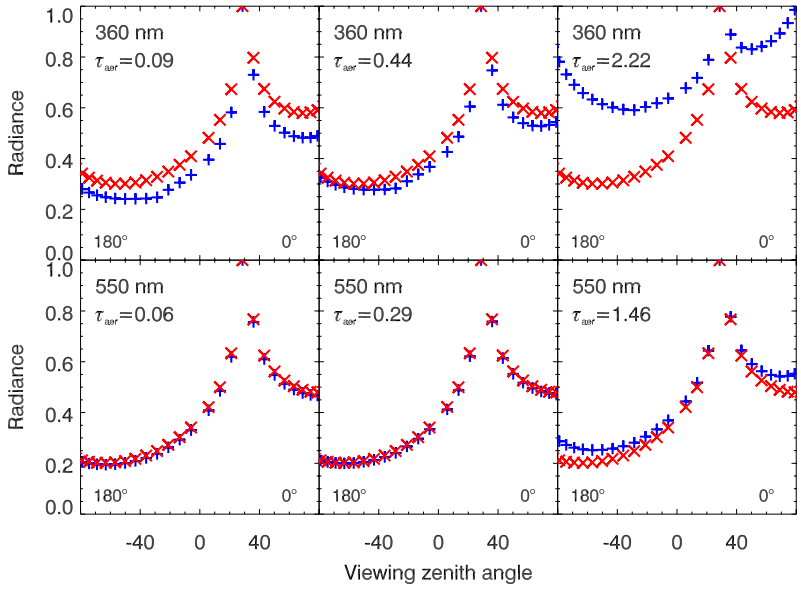

Figure 3: Comparison between the normalized upward radiance at the surface between the pure Rayleigh (x) and the aerosol loaded (+) atmosphere for a SZA of 30° and the two wavelengths of 360 and 550 nm using Hapke's BRDF.

greater contribution of the diffuse light to the total reflected radiation. At 550 nm, the reflected light is nearly completely described by the contribution of the direct light and changes of the diffuse light are therefore of secondary importance only.
Since satellite instruments measure the upward radiance at the top of the atmosphere we also investigate our model results for this quantity (Figure 4). At 360 nm we see nearly no

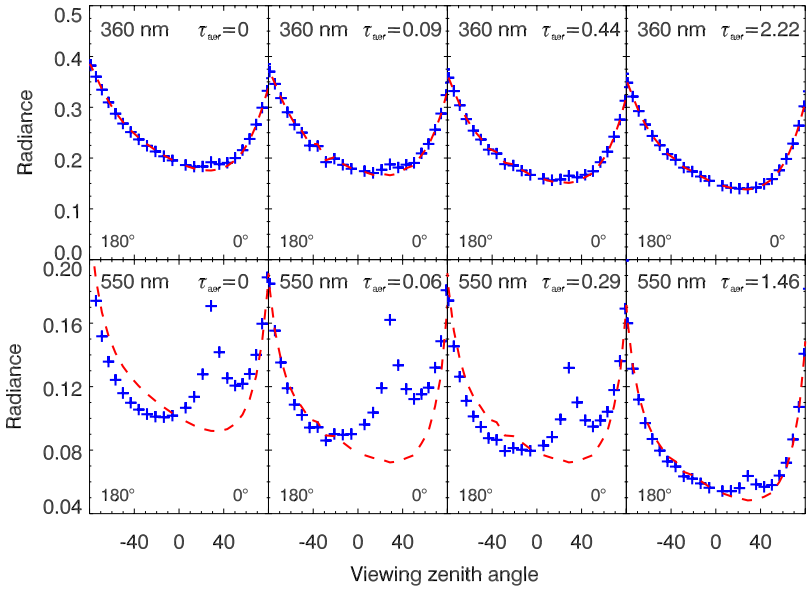

Figure 4: Upward radiance at the top of the atmosphere for a Lambertian surface (dashed line) and Hapke's BRDF (+). Results for the Rayleigh atmosphere ($\tau_{aer} = 0$) and three different aerosol optical depths are given at 360 and 550 nm. The SZA is 30°.

differences between a Lambertian surface and Hapke's BRDF. Only a little signal of the backscattering peak can be found at low aerosol optical thickness, but for large optical thickness as well as for a SZA of 60° (not shown) even this signature vanishes completely. The reason for this is that the upward radiance at the top of the atmosphere in case of strong Rayleigh scattering is determined from radiation which has never reached either the earth's surface or the aerosol layer existing within the four lowest model layers. This is confirmed by the fact that the results at 360 nm in Fig. 4 are nearly the same for all the optical thicknesses shown. The chosen BRDF is therefore of secondary importance at wavelengths with strong Rayleigh scattering.
At 550 nm, a clear difference between the two reflection types can be noticed from Figure 4 with a clear backscattering peak in case of Hapke's BRDF. For large viewing angles where the Rayleigh scattering is still dominating, both results approach each other. With increasing optical depth, the differences become less pronounced because the radiation reaching the earth's surface decreases (see Fig.2) and the reflected radiation is more weakend on the way to the top of the atmosphere.

5. Conclusion and outlook

Through the expansion of the surface boundary condition it is now possible to describe an angular dependent surface reflection, which is symmetric about the principal plane

within the Gauss-Seidel model for the applications given in the introduction. Therefore different BRDFs can be used. In case of Hapke's BRDF, it was shown that there are clear differences in comparison to the originally used Lambertian surface, especially in the region of the backscattering peak. This only has an effect on the upward radiance at the top of the atmosphere, if the Rayleigh scattering for the considered wavelength is not too strong. Otherwise the surface features are completely obscured by the atmosphere. A comparison of our model results with POLDER measurements from Bréon et al. (1997) over a Canadian boreal forest site, which have been not shown here, has led to satisfactory results and will be published elsewhere.

References

Anderson, G., S. Clough, F. Kneizys, J. Chetwynd, and E. Shettle, 1986: AFGL atmospheric constituent profiles (0-120 km). Technical Report AFGL-TR-86-0110, Air Force Geophys. Lab., Hanscom Air Force Base, Mass.

Barichello, L., R. Garcia, and C. Siewert, 1996: The Fourier decomposition for a radiative-transfer problem with an asymmetrically reflecting ground. *J. Quant. Spectrosc. Radiat. Transfer*, **56**(3), 363–371.

Bréon, F.-M., F. Maignan, M. Leroy, and I. Grant, 2001: Analysis of hot spot directional signatures measured from space. *J. Geophys. Res.*, **107**(D16), 4282–4296.

Bréon, F.-M., V. Vanderbilt, M. Leroy, P. Bicheron, C. Walthall, and J. Kalshoven, 1997: Evidence of hot spot directional signature from airborne POLDER measurements. *IEEE Trans. Geosc. Rem. Sens.*, **35**(2), 479–484.

Cox, C. and W. Munk, 1954: Measurements of the roughness of the sea surface from photographs of the sun's glitter. *J. Opt. Soc. Am.*, **44**(11), 838–850.

Diner, D. J., G. P. Asner, R. Davies, Y. Knyazikhin, J.-P. Nuller, A. W. Nolin, B. Pinty, C. B. Schaaf, and J. Stroeve, 1999: New directions in earth observation: Scientific applications of multiangle remote sensing. *Bull. Amer. Meteor. Soc.*, **80**(11), 2209–2228.

Hapke, B., 1981: Bidirectional reflectance spectroscopy. 1. Theory. *J. Geophys. Res.*, **86**(B4), 3039–3054.

Hasekamp, O. and J. Landgraf, 2002: A linearized vector radiative transfer model for atmospheric trace gas retrieval. *J. Quant. Spectrosc. Radiat. Transfer*, **75**, 221–238.

Henyey, L. and T. Greenstein, 1941: Diffuse radiation in the galaxy. *Astrophy. J.*, **93**, 70–83.

Herman, B. M. and S. R. Browning, 1965: A numerical solution to the equation of radiative transfer. *J. Atmos. Sci.*, **22**, 559–566.

Hungershöfer, K., 2001: Erweiterung der Bodenrandbedingung in einem Strahlungstransportmodell unter Verwendung einer anisotropnen Reflexionsfunktion. Diplomarbeit, Institut für Meteorologie, Johannes Gutenberg-Universiät Mainz.

Kaufman, Y. J., D. Tanré, and O. Boucher, 2002: A satellite view of aerosols in the climate system. *Nature*, **419**, 215–223.

Landgraf, J. and O. Hasekamp, 2002: Ozone profile retrieval from satellite measurements of nadir backscattered light in the ultraviolet of the solar spectrum. *Recent Res. Devel. Geophysics*, **4**, 157–189.

Landgraf, J., O. Hasekamp, M. A. Box, and T. Trautmann, 2001: A linearized radiative transfer model for ozone profile retrieval using the analytical forward-adjoint perturbation theory approach. *J. Geophys. Res.*, **106**(D21), 27291–27305.

Liou, K. N., 1992: *Radiation and Cloud Processes in the Atmosphere: Theory, Observation, and Modeling*. Oxford University Press, New York.

Meister, G., R. Wiemker, J. Bienlein, and H. Spitzer, 1996: In situ BRDF measurements of selected surface materials to improve analysis of remotely sensed multiangle imagery. In *Proceedings of the XVIII. Congress of the International Society of Photogrammetry and Remote Sensing ISPRS 1996*, 493–498.

Mérienne, M., F. Jenouvrier, and B. Coquart, 1995: The NO_2 absorption spectrum. I: Absorption cross-sections at ambient temperature in the 300-500 nm region. *J. Atmos. Chem.*, **20**, 281–297.

Minnaert, M., 1941: The reciprocity in lunar photometry. *Astrophy. J.*, **93**, 403–410.

Molina, L. and M. Molina, 1986: Absolute absorption cross sections of ozone in the 185- to 350-nm wavelength range. *J. Geophys. Res.*, **91**(D13), 14501–14508.

Nicodemus, F., 1970: Reflectance nomenclature and directional reflectance and emissivity. *Appl. Opt.*, **9**(6), 1474–1475.

Nicolet, M., 1984: On the molecular scattering in the terrestrial atmosphere: An empirical formula for its calculation in the homosphere. *Planet. Space Sci.*, **32**, 1467–1468.

Pinty, B. and D. Ramond, 1986: A simple bidirectional reflectance model for terrestrial surfaces. *J. Geophys. Res.*, **91**(D7), 7803–7808.

Pinty, B., M. M. Verstraete, and R. E. Dickinson, 1989: A physical model for predicting bidirectional reflectances over bare soil. *Rem. Sens. Env.*, **27**, 273–288.

Rahman, H., M.M.Verstraete, and B.Pinty, 1993: Coupled surface-atmosphere reflectance (CSAR) model: 2. Semiempirical surface model usable with NOAA advanced very high resolution radiometer data. *J. Geophys. Res.*, **98**(D11), 20791–20801.

Rothman, L., 1992: HITRAN spectroscopic data. *J. Quant. Spectrosc. Radiat. Transfer*, **48**, 497–507.

Shettle, E. P. and R. W. Fenn, 1979: Models for the aerosols of the lower atmosphere and the effects of humidity variations on their optical properties. Technical Report AFGL-TR-79-0214, Air Force Geophys. Lab., Hanscom Air Force Base, Mass.

Siegel, R. and J. R. Howell, 1981: *Thermal Radiation Heat Transfer*. McGraw-Hill Book Company, 2. edition.

Trautmann, T. and M. Box, 1995: Fast yet accurate net flux calculation for realistic atmospheres with variable aerosol loading. *J. Geophys. Res.*, **100**(D1), 1081–1092.

Trautmann, T., P. Elliot, and M. Box, 1992: Shortwave radiative effects of standard aerosol models: A perturbation approach. *Beitr. Phys. Atmosph.*, **65**(1), 59–78.

Verstraete, M., B. Pinty, and R. Dickinson, 1990: A physical model of the bidirectional reflectance of vegetation canopies 1. Theory. *J. Geophys. Res.*, **95**(D8), 11755–11765.

Walter, H., J. Landgraf, and T. Trautmann, 2002: Pseudo-spherical linearized radiative transfer model for trace gas profile retrieval. In *Proc. SPIE: Remote Sensing of Clouds and the Atmosphere VI*, Schaefer, K., Lado-Bordowsky, O., Comeron, A., Carleer, M. R., and Fender, J. S., Editors, Vol. 4539, 362–368.

Walthall, C., J. Norman, J. Welles, G. Campbell, and B. Blade, 1985: Simple equation to approximate the bidirectional reflectance from vegetation canopies and bare soil surfaces. *Appl. Opt.*, **24**(3), 383–387.

WMO, 1985: Atmospheric Ozone. World Meteorological Organization (WMO), Global Ozone Research and Monitoring Project, Report No.16, Geneva.

Woessner, P. and B. Hapke, 1987: Polarization of light scattered by clover. *Rem. Sens. Env.*, **21**, 243–261.

Woods, T., D. Prinz, G. Rottmann, J. London, P. Crane, R. Cebula, E. Hilsenrath, G. Brueckner, M. Andrews, O. White, M. VanHoosier, L. Floyd, L. Herring, B. Knapp, C. Pankratz, and P. Reiser, 1996: Validation of the UARS solar ultraviolet irradiances: Comparisons with the ATLAS 1 and 2 measurements. *J. Geophys. Res.*, **101**, 9541–9569.